Revisit of Typical Counterclockwise Atrial Flutter Wave in the ECG: Electroanatomic Studies on the Determinants of the Morphology

（通常型心房粗動の粗動波への再訪：3 次元マッピングを駆使した心電図波形解析）

申 請 者 弘前大学大学院医学研究科循環器腎臓内科学講座

氏 名　　佐々木　憲一

指導教授 若林　孝一

ABSTRACT

Background: Cavotricuspid isthmus-dependent counterclockwise atrial flutter (typical AFL) is characterized by negative saw-tooth morphology flutter wave (F-wave) in the inferior leads, which is classified as type 1 with purely negative F-wave without positive terminal deflection (PTD), type 2 with small PTD and type 3 with broad PTD. The determinants of these morphological differences remain to be elucidated.

Methods and Results: Of 72 patients (58 males, 65 ± 13 years) with typical AFL, 19 were classified as type 1 and 53 as types 2 and 3. We created electroanatomic map of the right atrium (RA) during AFL and determined which RA site activation corresponded to which F-wave component by analyzing the activation map. It was revealed that F-wave component from the nadir to terminal deflection point coincided with the cranio-caudal activation of the RA free wall (RAFW) in all types. The bipolar voltage map showed that type 1 had the greater extent of low voltage (<0.5 mV) area (LVA) in RAFW (39 ± 24%) than types 2 and 3 (4 ± 3%) (P <.0001), explaining the absence of PTD in type 1. In types 2 and 3, F-wave amplitude determining the PTD magnitude was highly correlated with the longitudinal distance between two points on RAFW corresponding to the nadir and peak of F-wave (r = 0.73, P <.0001).

Conclusions: Terminal positivity and amplitude of F-wave in typical AFL are primarily related to the RA free wall activity: negatively by the extent of LVA and positively by the longitudinal vector of activation.

INTRODUCTION

Cavotricuspid isthmus (CTI)-dependent counterclockwise (CCW) atrial flutter (AFL) (typical AFL) is characterized by the flutter wave (F-wave) with negative saw-tooth morphology in the inferior leads. It was reported that there were three types of F-wave including type 1 with purely negative F-wave inferiorly, type 2 with F-wave inferiorly with smaller positive terminal deflection, and type 3 with F-wave inferiorly with broader positive terminal deflection.[1] Negative deflection of F-wave is explained by caudo-cranial activation of the interatrial septum and the left atrium.[2-5] The upstroke and terminal component of F-wave in each of 3 types of AFL, however, have not been fully defined yet. The electroanatomic (EA) mapping is an effective tool for illustrating the conduction pattern of AFL, and enables us to correlate F-wave component with anatomical structures easily and interpret the arrhythmogenic substrate by analyzing the voltage map. With these benefits of EA mapping, we sought to determine the factors that affect the terminal component of F-wave, including positive terminal deflection in types 2 and 3, in the inferior leads in patients with typical AFL.

METHODS

Study Population

The study population was derived from the 205 consecutive patients referred to our institution for catheter ablation of AFL, which was proved CTI-dependent by the subsequent electrophysiological study, between March 2005 and November 2011. Among these patients, 25 with clockwise CTI-dependent AFL (reverse typical AFL), 7 patients with lower-loop reentry and 101 patients with typical AFL in whom EA mapping was not used for ablation and/or whose atrioventricular (AV) conduction ratio was $\leq$2 to 1 were excluded from the analysis. Therefore, this study consisted of the remaining 72 patients (mean age, 65 $\pm$ 13 years) with typical AFL who underwent radiofrequency ablation using EA mapping. Underlying heart disease was

present in 44 patients (61%) and concomitant atrial fibrillation in 38 (53%). None of the patients had undergone ablation of any arrhythmia including typical AFL prior to the study.

Electrophysiological Study

The study protocol was in agreement with the guidelines for clinical studies delineated by the Ethics Committee of our institution. All patients were studied in the post-absorptive non-sedated state after giving written informed consent to the electrophysiological study and catheter ablation. All antiarrhythmic drugs excluding amiodarone (with which 8 patients were treated) were discontinued for at least five half-lives before the procedure.

In all patients, a 7 Fr 20-pole, deflectable catheter (2-8-2 mm interelectrode spacing) (Inquiry H-Curve Diagnostic Catheter, St. Jude Medical, St. Paul, MN) was introduced via the femoral vein and placed along the tricuspid annulus (TA) to record the right atrial (RA) activation in the lateral wall and the CTI simultaneously. A 5 Fr decapolar catheter (2-8-2 mm interelectrode spacing) (Supreme CSL, St. Jude Medical) was inserted into the coronary sinus (CS) via the right internal jugular vein. In 20 patients, sinus rhythm was present at baseline, and programmed stimulation from the low RA or coronary sinus was performed to induce AFL. In the other 52, spontaneous AFL was present at baseline of the study. Consequently, typical AFL was studied in all patients. The CTI-dependence of AFL was confirmed by demonstrating concealed entrainment from the CTI with a post-pacing interval equal to the flutter cycle length and termination and elimination of AFL by CTI ablation.[6] Studies were recorded on optical disk using ComboLab system (GE Healthcare UK Ltd, Buckinghamshire, England).

ECG Analysis

In all patients, 12-lead ECG during episodes of typical AFL was recorded and read at 25 mm/s sweep speed with a filter setting of 0.05 Hz (high pass) and 100 Hz (low pass). The morphology of F-wave was analyzed in the ECG showing more than or equal to 3 to 1 AV conduction to avoid superimposition of the F-wave on the T wave. In the present study, F-wave

morphology in the inferior leads was evaluated. Milliez et al previously classified F-wave morphology into three types including type1 showing F- or f- morphology, type 2 F-/f+, and type 3 f-/F+ (Figure 1). F- or f- in type 1 indicates monophasic F-wave. On the other hand, both types 2 and 3 show biphasic F-wave, and these types depend on the differences in the amplitude and duration of the initial negative and terminal positive components (F-/f+ and f-/F+, respectively). In the present study, we focused on the RA parts relating to each of F-wave components including the downslope and upslope of the negative component and following terminal positive component seen in types 2 and 3. Thus, we sought to determine which site of RA activation corresponded to which component of F-wave. For this purpose, we categorized F-waves into type A with monophasic morphology (Milliez's type 1) and type B biphasic (Milliez's types 2 and 3). To further characterize type B biphasic F-wave, we measured the amplitude of F-wave (from the nadir to the peak of F-wave), and examined the influential factor to the amplitude.

EA Mapping Study

In all patients, EA mapping of the RA was performed during AFL with the use of 3-dimensional (3D) mapping system (CARTO or CARTO XP, Biosense-Webster, Diamond Bar, CA) and a 4-mm tip quadripolar mapping catheter (Navistar, Biosense-Webster). After creation of the activation map of the whole RA by the sampling from 208 ± 89 points, we examined the relationship between the RA activation and ECG component of F-wave in the inferior leads by projecting F-wave on the map (Figure 2A).

In each patient, bipolar voltage map was created by applying the color scale. The color "gray" represents the points with the peak-to-peak electrogram amplitude <0.03 mV which was defined as "scar lesion", "red to blue" represents the points with the amplitude <0.5 mV which was defined as "low voltage lesion" and "purple" represents the points with the amplitude ≥0.5 mV which was defined as a "normal voltage area". The RA surface area was calculated by an

area measurement tool incorporated with CARTO system. We first defined the RA wall area, anterior to the posterior double potential line and lateral to the vertical-line drawn at 12 o'clock of the TA in the LAO view as total RA free wall area (Figure 2B). Then, we measured the low voltage area (LVA) with the bipolar voltage <0.5 mV in total RA free wall area and calculated the percentage of LVA in total RA free wall area.

Analysis of CS Catheter Electrograms

The present study was done without detailed evaluation of the LA activation pattern during typical AFL because EA mapping of the LA was not available. As a surrogate marker for a part of LA activation, we analyzed the relative timing of the CS atrial electrograms to AFL cycle and examined which portion of F-wave the CS activation corresponded with.

Catheter Ablation

In all patients, CTI was ablated using an 8-mm tip catheter (Blazer, Boston Scientific, Natick, MA, or Ablaze Fantasista, Japan Lifeline, Tokyo, Japan). The energy setting was as follows: temperature limit, 60 degree Centigrade; power, 50 W. The endpoint of ablation was the creation of bidirectional CTI block.

Statistical Analysis

Continuous variables are expressed as mean ± standard deviation. Comparison of categorical variables was performed by the Fisher exact test and that of continuous variables by Student *t* test. Linear regression studies were performed to investigate correlations between parameters. $P < 0.05$ was considered statistically significant.

RESULTS

Baseline Characteristics (Table 1)

Of the 72 patients, 19 (26%) showed monophasic F-wave (type A), and the other 53 (74%) biphasic (type B). Any of the mean age, the incidence of concomitant atrial fibrillation,

and the echocardiographic parameters was not significantly different between the two types. All of type A patients had underlying, structural heart disease, while 40% of type B patients had (P <0.001). Among type A patients, 15 (79%) had prior cardiac surgery. Flutter cycle length in type A (266 ± 35 msec) was longer than those in type B (239 ± 26 msec) (P <0.001). The mean F-wave amplitude in aVF lead was 0.15 ± 0.05 mV in type A and 0.25 ± 0.08 in type B (P <0.01).

RA Activation Site Corresponding to Each F-wave Component

Activation and propagation maps revealed the consistent correlation between each F-wave component and activation site in the RA. In type B patients, F-wave was divided into 4 components (Figure 3A). The first part with gently downward slope corresponded to the activation in the CTI and CS ostial region. The second part with negative deflection corresponded to that in the interatrial septum. The third part with upstroke corresponded to that in the upper part of RA free wall (from 0 o'clock to 8 in a counterclockwise direction around TA in the LAO view), and the fourth part with terminal deflection did to that in the lower part of RA free wall (A representative RA activation pattern corresponding to each F-wave component is shown Figure 3B). In type A patients, F-wave was divided into three components, as the third and fourth parts were combined together. These relationships between the F-wave components and RA activation sites were observed in 70 (97%) of the study patients. Thus, the F-wave components from the nadir through the top of the upstroke to the terminal deflection point (yellow and green components in Figure 3A) were found to correspond to the RA free wall activation.

Effect of the Extent of LVA in the RA Free Wall on F-wave Morphology and Conduction Velocity

Mean bipolar voltage of the whole RA points was 0.8 ± 0.3 mV in type A and 2.5 ± 1.0 mV in type B (P <.0001). Bipolar voltage map revealed the significant influence of LVA in the

RA free wall to F-wave morphology (Figure 4). There was no difference in the total area of the RA free wall between type A (70 ± 16cm^2) and type B (73 ± 16cm^2). However, the LVA was significantly greater in type A (29 ± 19cm^2) than in type B (3 ± 2cm^2). Accordingly, the percentage of LVA in the RA free wall was significantly greater in type A (39 ± 24%) than in type B (4 ± 3%) (P <.0001).

Further, the conduction velocity along the RA free wall measured by dividing the length between the 2 points arbitrarily selected at the upper and lower parts in the RA free wall by the time interval was significantly smaller in type A (0.61 ± 0.12 m/sec) than in type B (1.12 ± 0.27 m/sec) (P <0.01). These values may not necessarily be accurate since the path of the activation wavefront could not be determined precisely. However, such a difference in the conduction velocity may be related to smooth F-wave upstroke and longer flutter cycle length in type A.

The Relationship between the Extent of LVA and F-wave Amplitude

We initially assumed that F-wave with high-amplitude or broad positive terminal deflection was associated with a greater normal voltage area in the RA free wall. As shown in Figure 5A, however, F-wave amplitude was not necessarily correlated to the voltage in the RA free wall. Figure 5B shows the correlation between the extent of LVA in the RA free wall and F-wave amplitude in type B. The amplitude of F-wave was not related to the extent of LVA in the RA free wall.

The Relationship between the Longitudinal Vector of the RA Free Wall Activation and F-wave Amplitude

As mentioned before, the RA wall was activated in a counterclockwise direction from 0 o'clock to 8 around TA in the LAO view during the interval of nadir to peak of type B F-wave. The more caudal the vector of activation is, the higher the amplitude in the inferior leads. Based on this concept, we selected 3 to 5 pairs of points on the RA free wall in the RAO view through

which the activation wavefront passed. We defined the points positioned most cranially as the starting points, and the ones corresponding to the peak of F-wave as the terminal points. Then we measured the vertical distance between the starting and the terminal points and defined it as longitudinal distance (LD) (Figure 6A and 6B). We sampled 3 to 5 LDs and calculated the average. The amplitude of F-wave was highly correlated to the distance ($r = 0.73$, $P < .0001$) (Figure 6C).

The Timing of Activation of the CS Electrograms

The interval of the activation from the proximal to distal electrodes in the CS catheter occupied less than half of tachycardia cycle length (41 ± 6%). The F-wave components corresponding to this time interval were the last part of gentle downslope and the initial part of negative deflection, which were consistent with the activation of CS ostium and interatrial septum, as showed before.

Catheter Ablation and Follow-up (Table 2)

CTI was successfully ablated in all patients. In 7 type A AFL patients (37%), atypical, CTI-independent AFL including upper loop reentry (6 patients) and free wall scar-related reentry (one) was induced following CTI ablation, and was also ablated successfully. There were no complications during the procedure. During the follow-up of 42 ± 23 months, three patients (one with type A and 2 with type B) had a recurrence of typical AFL.

DISCUSSION

Major Findings

With the use of EA mapping, we investigated the correlation between each of the ECG components of F-wave in typical AFL and the activation site in the RA. We sought the determinants for F-wave morphology variation, especially the terminal positivity by analyzing the bipolar voltage map during AFL and RA free wall activation in the longitudinal direction. It

was revealed that whether a positive terminal deflection is present in the F-wave in the inferior leads depends on the extent of LVA in the RA free wall, and F-wave amplitude, which may be a determinant of the size of positive terminal deflection, depends on the longitudinally-directed vector of the RA free wall activation. To our best knowledge, this is the first study that quantitatively demonstrated the determinants of the extent of the terminal positivity in the F-wave.

Projecting F-wave on EA Map

Previous studies analyzed the relationships between endocardial activation and surface ECG without EA mapping.[2-5] With the use of 62-lead body surface mapping, SippensGroenewegen et al reported that the positive terminal deflection in the inferior leads could be caused by late cranio-caudal activation of the lateral RA wall.[7] By recording multiple electrograms in the RA using a basket catheter, Ndrepepa et al showed that the activation of the lateral wall of RA coincided with the upstroke component in the inferior leads.[3] We corroborated these findings with the use of EA map, which easily allowed us to correlate the time course of the surface ECG with the endocardial activation. We analyzed the points on the EA activation map which corresponded to each of the components with F-wave. The results showed that the upstroke of F-wave and terminal deflection (yellow and green colors in Figure 3A) represented cranio-caudal activation in the RA free wall.

Cavotricuspid Isthmus

Allessie et al suggested that the electrically quiescent part in the flutter cycle was due to activation through a narrow isthmus of the atrial myocardium that was a part of the macroreentrant circuit and was responsible for the isoelectric segment on the surface ECG.[8] SippensGroenewegen et al also found that the activation of the small muscle mass of the medial part of the subeustachian isthmus generated a low amount of electromotive forces, which resulted in a period of relative electrical silence on the surface ECG.[7] Similarly, we found that

the initial part of negative deflections showing gradual voltage decline coincided with activation of the subeustachian isthmus with EA mapping.

LVA on the RA Free Wall as the First Determinant of F-wave Morphology Variation

Milliez et al categorized F-wave morphology into three types and reported that a positive component of the F-wave in the inferior leads during typical AFL was associated with the LA enlargement, heart disease and atrial fibrillation.[1] Even though their classification appears simple, it might be difficult to compare the voltage of the terminal positivity (broad or small) and differentiate types 2 (F-/f+) and 3 (f-/F+) clearly, because of the arbitrariness of delineating horizontal line on the ECG separating negative and positive parts. Therefore, in the present study, we first categorized inferior F-wave morphology into two types (type A = type 1 by Milliez's classification and type B = types 2 and 3) based on the overall terminal morphology (monophasic or biphasic). We found no significant differences between the patient profiles in the two types with regard to age, concomitant atrial fibrillation, and LA enlargement, but found a higher incidence of the underlying heart disease in patients with type A F-wave (Milliez's type 1). We speculated that the underlying heart disease might be associated with the damaged myocardium including the RA free wall, and thus with the absence of positive terminal deflection in F-wave. Patients with prior cardiac surgery had surgical scar caused by atriotomy or cannulation on the RA free wall. Especially, the patients with atrial septal defect and Ebstein anomaly, which caused the RA enlargement by itself, had large LVA. In fact, this study revealed that type A had a greater extent of LVA than the other, which led to the absence of the positive component with F-wave. It also allowed the RA activation to be prolonged, which contributed to a longer flutter cycle length in type A AFL.

With regard to type B (biphasic) F-wave, bipolar voltage in the RA free wall little affected the morphology of F-wave. As shown in Figure 5, F-wave amplitude was not related to the extent of LVA. In fact, type B with biphasic F-wave had almost normal voltage in the RA

wall except the postero-inferior wall of the RA around inferior vena cava. Thus, the morphological difference in the biphasic F-wave was suggested to be determined by another factor, as described hereafter.

Longitudinal Vector of the RA Free Wall Activation as the Second Determinant of F-wave Morphology Variation

The amplitude in any ECG lead reflects the extent of the vector along the lead on which the heart vector is projected.[9] This study revealed that the longitudinal distance between the two points on the RA free wall corresponding to the nadir and peak of F-wave (lead aVF vector) strongly correlated with F-wave amplitude in the inferior leads during typical AFL. The magnitude of amplitude seems to be related to the visual variation of positive terminal deflection, based on which Milliez et al classified biphasic F-waves of typical AFL into two types (type 2 with F-/f+ and type 3 with f-/F+).[1] In fact, the size of positive terminal deflection does not reflect the condition of the atrial myocardium (normal or damaged) but was determined by the longitudinally directed vector of the RA free wall activation. If the RA contour is oval in the LAO view, the longitudinal distance of the RA free wall activation is short, which results in low-amplitude F-wave with small positive terminal deflection. If the RA is taller, the longitudinal distance of the RA free wall activation is long, which makes the amplitude of F-wave higher and positive terminal deflection broader. There may be at least two possible reasons why the RA contour varies among the patients with type B F-wave. The first is because the RA contour is affected by the surrounding structure, especially the ascending aorta. If the RA is compressed medially by the dilated or deviated aorta, the contour is oval in the LAO view and the lateral area in RA free wall is small. The second is because the axis of the heart including RA is deviated in a dorsoventral direction congenitally or postnatally.

Prior Studies

We showed both consistent and inconsistent findings with those in the prior studies.

Our EA mapping findings on the relationship between the F-wave components and RA endocardial activation sites were consistent with those by Ndrepepa et al and SippensGroenewegen et al.[3, 7] Although the reason is not clear, there are inconsistency between Milliez's findings[1] and ours. They analyzed typical AFL mainly by surface 12-lead ECG and patient clinical characteristics without EA mapping system, and there is a possibility that lower-loop reentry AFL had been included in type 1 AFL which they analyzed. The surface ECG pattern is very similar between lower-loop reentry and typical AFL except for decreased amplitude of the late positive waves in the inferior leads.[10] Chugh et al reported that F-waves in the inferior leads were upright after LA ablation of atrial fibrillation because of a significant reduction in bipolar LA voltage.[5] We postulate that Milliez's type 3 F-wave corresponds to this type of F-wave. This is because impaired LA voltage leads to loss of negative deflection and positive deflection becomes relatively broad. We also encountered such cases, in one of which LA was rudimentary. In another case, LA bipolar voltage was found to be very low by EA mapping during LA-AFL which was done later.

Yuniadi et al recognized the influence of atrial propagation pattern to the ECG and concluded that F-wave polarity and voltage measurement in lead I could differentiate reverse typical AFL from upper loop reentry.[11] In the reentry circuit of atypical AFL such as upper loop and RA free wall reentry, abnormal RA tissue represented by unipolar low voltage electrogram was shown to be characterized by slow conduction and serve as critical isthmus.[12]

Study Limitations

In this study, EA mapping of the LA during typical AFL was not done. The details of interatrial conduction and the whole LA activation are necessary to determine how they affect F-wave morphology. We substituted electrograms in the CS catheter for a part of LA activation, the interval of which occupied only less than half of tachycardia cycle length and was corresponded to the initial part of the negative deflection of F-wave. This finding corroborated

Chugh's report in which they underwent LA mapping by EA mapping system during typical AFL and concluded that the whole LA activation coincided not with positive but negative deflection.[5] The difference of the longitudinal vector of the RA free wall activation during typical AFL may be produced by the RA contour, but we could not verify this RA contour variation by the right atriography or 3D computed tomography image in every case.

Conclusions

The present study implicates that whether a positive terminal deflection is present in F-wave depends on the voltage of RA free wall: in the patients with impaired RA free wall, the terminal positivity is absent, resulting in the monophasic negative F-wave. The extent of terminal positivity is determined by the longitudinally directed vector of the RA free wall activation.

DISCLOSURES

None.

REFERENCES

1. Milliez P, Richardson AW, Ogundu O, Zimetbaum PJ, Papageorgiou P, Josephson ME. Variable electrocardiographic characteristics of isthmus-dependent atrial flutter. *J Am Coll Cardiol*. 2002;40:1125-1132.

2. Okumura K, Plumb VJ, Page PL, Waldo AL. Atrial activation sequence during atrial flutter in the canine pericarditis model and its effect on the polarity of the flutter wave in the electrocardiogram. *J Am Coll Cardiol*. 1991;17:509-518.

3. Ndrepepa G, Zrenner B, Deisenhofer I, Karch M, Schneider M, Schreieck J, Schmitt C. Relationship between surface electrocardiogram characteristics and endocardial activation sequence in patients with typical atrial flutter. *Z Kardiol*. 2000;89:527-537.

4. Rodriguez L-M, Timmermans C, Nabar A, Hofstra L, Wellens HJJ. Biatrial activation in isthmus-dependent atrial flutter. *Circulation*. 2001;104:2545-2550.

5. Chugh A, Latcamsetty R, Oral H, Elmouchi D, Tschopp D, Reich S, Igic P, Lemerand T, Good E, Bogun F, Pelosi FJ, Morady F. Characteristics of cavotricuspid isthmus-dependent atrial flutter after left atrial ablation of atrial fibrillation. *Circulation*. 2006;113:609-615.

6. Saoudi N, Cosio F, Waldo A, Chen SA, Iesaka Y, Lesh M, Saksena S, Salerno J, Schoels W. Classification of atrial flutter and regular atrial tachycardia according to electrophysiologic mechanism and anatomic bases: a statement from a joint expert group from the Working Group of Arrhythmias of the European Society of Cardiology and the North American Society of Pacing and Electrophysiology. *J Cardiovasc Electrophysiol*. 2001;12:852-856.

7. SippensGroenewegen A, Lesh MD, Roithinger FX, Ellis WS, Steiner PR, Saxon LA, Lee RJ, Scheinman MM. Body surface mapping of counterclockwise and clockwise typical atrial flutter: a comparative analysis with endocardial activation sequence mapping. *J Am Coll Cardiol*. 2000;35:1276-1287.

8. Allesie MA, Lammers WJ, Bonke IM, Hollen J. Intra-atrial reentry as a mechanism for atrial flutter induced by acetylcholine and rapid pacing in the dog. *Circulation*. 1984;70:123-135.

9. Mirvis DM and Goldberger AL. Electrocardiography. In: Libby P, Bonow RO, Mann DL, and Zipes DP, eds. *Braunwald's heart disease: A textbook of cardiovascular medicine*. 8th ed. Philadelphia, PA:Saunders; 2008:pp.149-189.

10. Bochoeyer A, Yang Y, Cheng J, Lee RJ, Keung EC, Marrouche NF, Natale A, Shieinman MM. Surface electrocardiographic characteristics of right and left atrial flutter. *Circulation*. 2003;108:60-66.

11. Yuniadi Y, Tai CT, Lee KT, Huang BH, Lin YJ, Higa S, Liu TY, et al. A new electrocardiographic algorithm to differentiate upper loop re-entry from reverse typical atrial flutter. *J Am Coll Cardiol*. 2005;46:524-528.

12. Huang JL, Tai CT, Lin YJ, Huang BH, Lee KT, Higa S, Yuniadi Y, et al. Substrate mapping to detect abnormal atrial endocardium with slow conduction in patients with atypical right atrial flutter. *J Am Coll Cardiol*. 2006;48:492-498.

FIGURE LEGENDS

Figure 1. This figure shows schemas of three types of variable typical atrial flutter wave (F-wave) morphologies in the inferior leads into which Milliez et al categorized. The first (type1) is monophasic negative F-wave (F- or f-); the second (type 2), biphasic predominantly negative F-wave with a small terminal positive component (F-/f+); and the third (type 3), biphasic predominantly positive F-wave with a small initial negative component (f-/F+).

Figure 2. A, Projection of F-wave in the inferior leads on activation map. (left panel) The nadir of F-wave (red circle) corresponds to the activation of upper portion of interatrial septum (arrow). (right panel) The peak of F-wave (red circle) corresponds to the activation of lateral part of the right atrial (RA) free wall (arrow). **B,** Area of total RA free wall and low voltage (<0.5 mV) area (LVA) within it. (left panel) Right anterior oblique (RAO) view of the RA. (right panel) Left anterior oblique (LAO) view of the RA. Sky blue tags represent double potentials; gray tags, scar area; pink tags, tricuspid annulus; and pale pink tags, fragmented potentials. TA indicates tricuspid annulus.

Figure 3. The relationship between each of F-wave components and activated site in the right atrium. **A,** F-wave in the inferior leads including gently downward slope (blue), negative deflection (red), steep upstroke (yellow), and terminal deflection (green). **B,** The colored curved-arrows correspond to the 4 portions of F-wave with the same color (in Figure A). CS indicates coronary sinus; TA, tricuspid annulus.

Figure 4. The effect of low voltage (<0.5 mV) area (LVA) in the right atrial (RA) free wall on F-wave morphology. **A,** There was no difference in the total RA free wall area between the two types. **B,** LVA in type A was significantly greater than that in type B, resulting in the greater

percentage of LVA to total RA free wall area in type A than in type B.

Figure 5. A, Variation in the amplitude of type B (biphasic) F-wave. AFL 1 (upper panel) shows F-wave with higher amplitude than AFL 2 (lower panel), although the bipolar voltage in the right atrial (RA) free wall is normal (≥0.5 mV) in both AFLs. **B,** Relationship between the amplitude of type B F-wave (in lead aVF) and the extent of low voltage (<0.5 mV) area (LVA) in the RA free wall. LVA indicates low voltage area.

Figure 6. A and B, Measurement of the longitudinal distance between 4 pairs of the points on the RA free wall. In the propagation map, we sampled the points on the RA wall through which the wavefront passed during the interval corresponding to the nadir and peak of type B F-wave (Figure A). Among these points, 3 to 5 points positioned most cranially in the RAO view were selected and defined as the starting points (red circles). Then, the points vertical to the starting points and corresponding to the peak of F-wave were selected and defined as the terminal points (white circles). We measured the distance between each pair of the points (Figure B). **C,** Relationship between type B F-wave amplitude (in lead aVF) and longitudinal distance between the two points in each pair. Sky blue tags represent double potentials; gray tags, scar area. TA indicates tricuspid annulus.

Figure 1.

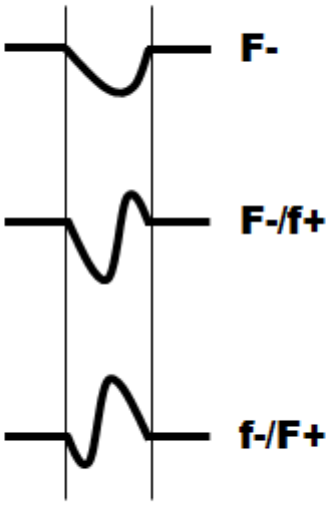

.

Figure 2. A

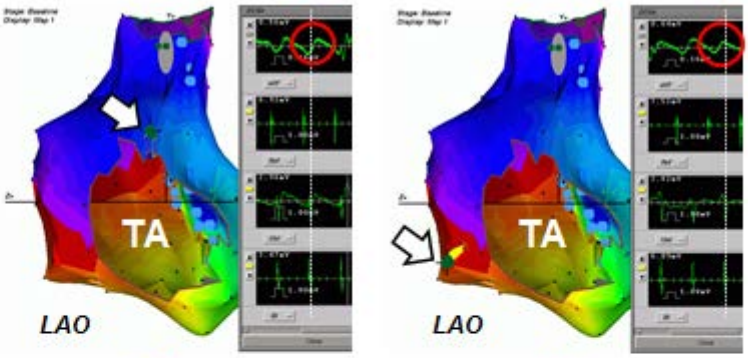

B

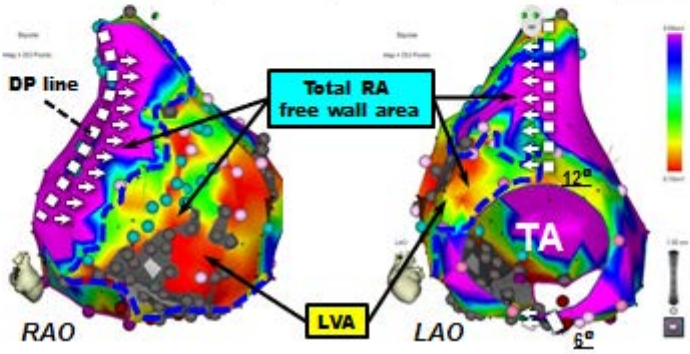

Figure 3.

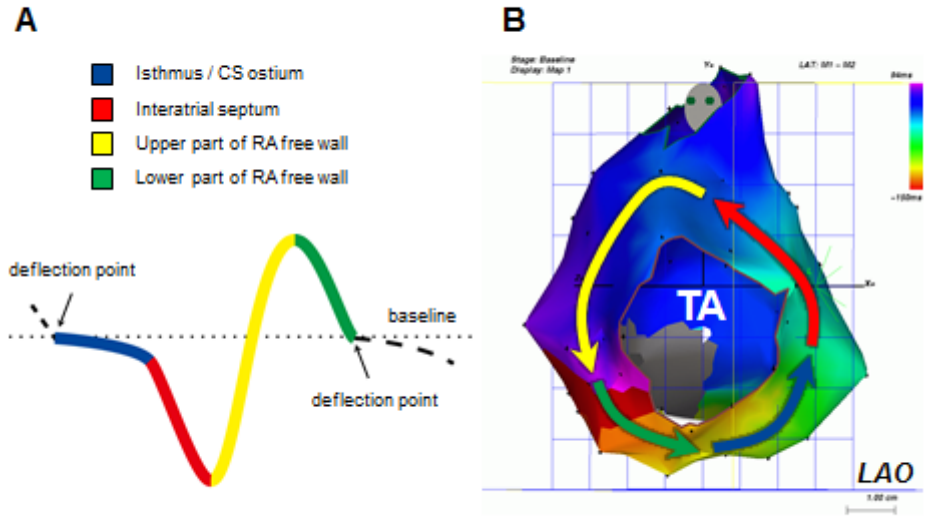

Figure 4.

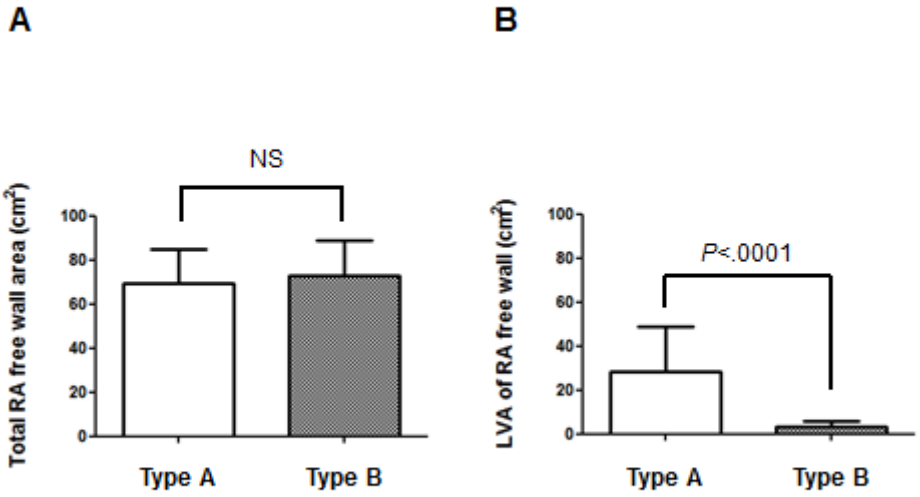

Figure 5. A

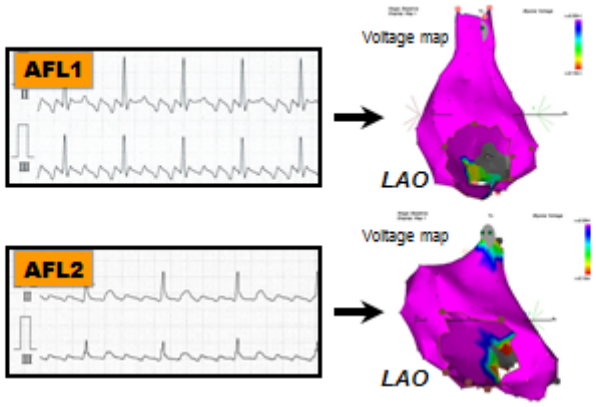

B

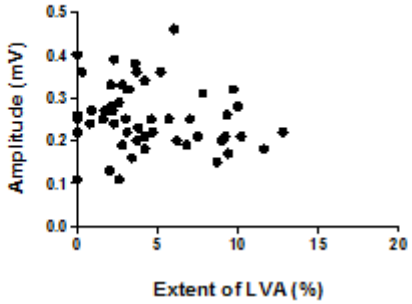

Figure 6.

A

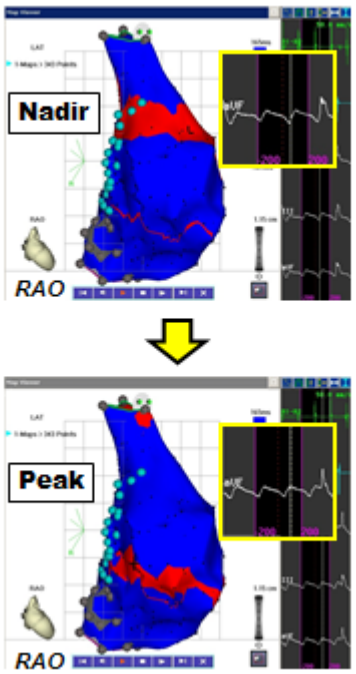

B

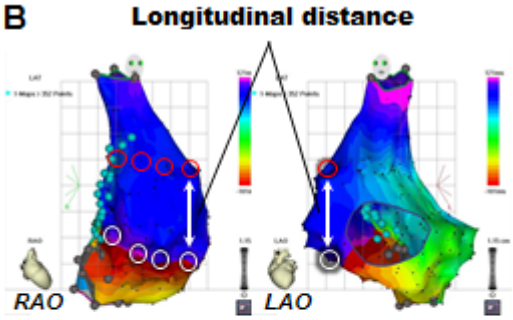

C

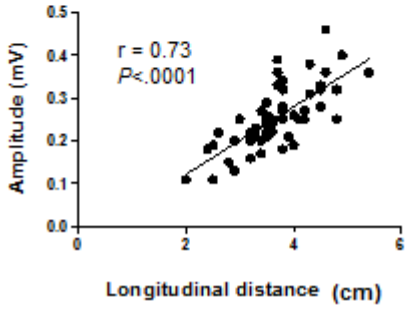

Table 1. Clinical Characteristics of Patients with Two Types of Typical Atrial Flutter

	Monophasic = Type A (n=19)	Biphasic = Type B (n=53)
Age (years)	62 ± 16	66 ± 12
Male, n (%)	10 (53)	48 (91)*
Hypertension, n (%)	1 (5)	26 (49)†
History of atrial fibrillation, n (%)	8 (42)	30 (57)
Structural heart disease, n (%)	19 (100)†	21 (40)
Heart failure due to TIC, n (%)	3 (16)	5 (9)
Coronary artery disease, n (%)	2 (11)	10 (19)
Dilated/hypertrophic cardiomyopathy, n (%)	0 (0)	4 (8)
Congenital/valvular disease, n (%)	14 (74)	2 (4)
Prior cardiac surgery, n (%)	15 (79)†	3 (6)
Coronary artery bypass graft, n (%)	0 (0)	2 (4)
Valve replacement/plasty, n (%)	4 (21)	1 (2)
ASD repair, n (%)	6 (32)	0 (0)
Others (Ebstein/TOF/CP repair)	5 (26)	0 (0)
LV ejection fraction (%)	53 ± 11	57 ± 14
LA diameter (mm)	41 ± 6	41 ± 8
Flutter cycle length (msec)	286 ± 35†	239 ± 26

TIC indicates tachycardia-induced cardiomyopathy; ASD, atrial septal defect; TOF, tetralogy of Fallot; CP, constrictive pericarditis; LV, left ventricular; and LA, left atrial. *P<0.01; †P <0.001

Table 2. Procedure Details of Catheter Ablation

	Monophasic = Type A (n=19)	Biphasic = Type B (n=53)
Total procedure time (min)	170 ± 55*	139 ± 36
Ablation time for CTI (min)	9 ± 7	11 ± 9
Recurrence of typical AFL, n (%)	1 (5)	2 (4)
Incidence of other types of RA-AFL, n (%)	7 (37)†	0 (0)
Follow-up time (months)	43 ± 26	42 ± 22

CTI indicates cavotricuspid isthmus; AFL, atrial flutter; and RA, right atrium. *P <0.05; †P <0.01